The Design of a Novel Hot Gas Filter Unit

A.G. Konstandopoulos, G. Macheridou, E. Skaperdas
Foundation for Research and Technology Hellas
Chemical Process Engineering Research Institute
P.O. Box 361, Thermi, Thessaloniki 57001, Greece

P. Stobbe, L. Johannesen
NOTOX International S.A., Sandtoften 10
DK-2820, Gentofte, Denmark

J. Hoej
Department of Chemistry, Materials Science Group
Technical University of Denmark, DK-2800 Lyngby, Denmark

Abstract

State of the art hot gas particle clean-up technology is typically based on ceramic candle filters (rigid and soft), and to a lesser on smaller, one piece honeycomb cross flow filters. The technology is still in states far from providing reliable and cost effective particulate removal from hot gases. Major problem areas involve : mechanical failure due to ash particle bridging, filter thermal stability and material compatibility issues, system price due to a high candle filter weight and manufacturing cost, and an appreciable pressure drop, to name a few.

The objective of the current research is to develop a compact hot gas particulate clean-up system by integrating specifically tailored, advanced high temperature ceramic materials into a novel, and cost effective filter design, so as to overcome problems with current candle technology. The proposed hot gas filter system is constructed combining individual filter elements to create an assembled honeycomb structure.

The filter system has been simulated computationally with respect to its structural and flow characteristics during normal operation and cleaning procedure. In addition, filter coupons from appropriate ceramic materials have been constructed and tested in a flow rig with respect to permeability, to provide data for the optimal pilot-scale manufacturing of a prototype unit.

Keywords : ceramic filter, single filter element, modeling, silicon carbide, Darcy's law, pulse cleaning.

1. Introduction

Advanced power generation cycles from solid fuels can contribute significantly to future European energy security and require particle-clean combustion/gasification product gases at high temperatures in order to achieve at the same time significant energy efficiency and environmental benefits [1-3]. State-of-the-art hot gas particle clean-up technology is typically based on ceramic candle filters (rigid and soft), and to a lesser extent on smaller, one piece honeycomb cross-flow filters [4-5]. The technology is still in a stage far from providing reliable and cost-effective particulate removal from hot gases. Major problem areas involve: mechanical failure due to ash particle bridging, filter thermal stability and materials compatibility issues, system price due to high candle filter weight and manufacturing cost and appreciable pressure drop, to name a few. Rigid candles generally have thick walls (>10 mm), determined by the often low material strength and the porosity requirements for acceptable pressure drop. Ceramic candles having a high weight, increase the support system weight considerably. In addition, ceramic rigid candles are prone to breakage as they have relatively low mechanical strength and are often put under stress by uncontrolled particle build-up between two or more candles as well as by thermal cycling. Rigid candles are generally produced by using clay bonded ceramic grains sintered in an oxidizing atmosphere. The clay limits or reduces the mechanical strength of the candles. Soft filter candles suffer from low mechanical strength. These filter elements are made of vacuum formed ceramic fibers, held together with inorganic binders in thick walls and formed into candles. Fibers from down-stream areas of the filters are prone to loosening and being carried away during the cleaning process and exhausted with the cleaned gas to the environment. As alternative to candle filters cross-flow monolithic filters have also been investigated [4-5]. These are only possible to be manufactured in rather small substrate sizes. Therefore, great numbers are needed for large filter units causing complicated installation problems. The objective of the present study is to investigate a novel compact and cost-effective hot gas filter design with the following characteristics compared to a similarly sized candle-based system:

1.Half the system weight for the same volume
2.Considerably reduced system price
3.More than double the filtration surface to volume ratio
4.Considerably lower pressure drop with high filtration efficiency
5.Fewer problems in terms of mechanical failure due to ash bridging

2. Filter Design Concept

At the heart of the new proposed hot gas filter system there is a filter unit comprising an assembled honeycomb structure (Fig.1). By assembling many individual filter elements (channels) into one or several large structures the proposed rigid, low density filter units are to be viewed as giant honeycomb structures. By enclosing many separate elements in a container, it becomes possible to obtain the same behaviour as that of a one piece fabricated cross-flow honeycomb structure. All mechanical forces are transferred through the walls to the canning container. The dimensions of a giant assembled honeycomb unit could reach as much as 3 meters in length and 10 meters in diameter, with as high as 190 m^2/m^3 filtration surface/filter volume. The unit described hereby can make more efficient use of the volume taken up by filtering systems using appropriate packaging technology. The weight reduction is important for any system where load transients are common, such as emergency and peak-power electrical plants. It is believed that the total system weight can be reduced to at least half the weight of candle based systems. The filter cleaning can be effected with jet back-pulsing similar to candle filters.

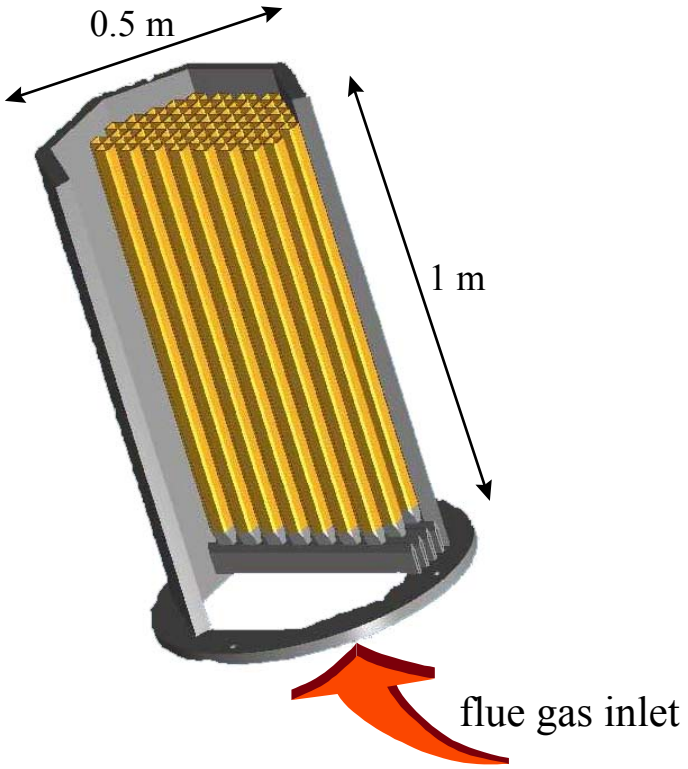

Figure 1 : Solid model of pilot-scale assembled honeycomb filter

In the present study we undertake a preliminary design of the filter element employing where appropriate Computational Fluid Dynamics (CFD) tools and analytical modeling in order to assess the feasibility, advantages and application range of the new filter concept. In addition, we describe the commissioning of a new hot gas filter laboratory testing rig and preliminary permeability

experiments with coupons from ceramic materials, that will be employed for the filter construction.

3. Flow Design

3.1 CFD modeling

The filter as seen in Fig. 1 consists of several ceramic channels, with a square cross section and one end blocked, assembled together thus forming inlet and outlet channels. To examine in detail the flow characteristics of the assembled filter it is convenient to study first the flow behavior of an individual channel, exploiting the symmetry of the problem. A commercial CFD package [6] was used for the analysis of the flow of a single channel of the assembled filter under normal operation and under pulse jet cleaning. The flue gas was assumed to have the properties of air at the filter operational conditions listed in Table 1.

Table 1 : Filter geometry and flow parameters used for the CFD simulations

Operational Pressure (atm)	10	Assembled filter height, L (m)	1.0
Operational temperature (°C)	600	Assembled filter diameter, D (m)	0.5
Density, ρ (kg/m^3)	4.0	Assembled filter volume, V (m^3)	0.196
Viscosity, μ (kg/m sec)	3.8x10^{-5}	Filtration area, A_{filt} (m^2)	9.52
Filtration velocity, U_{filt} (cm/sec)	4.0	Filtration area/Volume (m^2/m^3)	48.6
Channel inlet velocity, U_1 (m/sec)	4.7	Actual volume flow rate, Q (m^3/hr)	1370

Each square channel of the filter has an external width of 40 mm and a 3 mm thickness. The assembled prototype filter has the characteristics listed in Table 1. In the following paragraphs we describe briefly the CFD computations performed.

3.1.1 Steady state simulations

To simulate the normal operation of the filter a steady state calculation is performed. The flow is 3-D, steady and turbulent as the inlet Reynolds number based on the channel width is approximately 17000. The effects of turbulence are simulated by the ReNormalization Group (RNG) k-ε model [6], and a 5% turbulence intensity is specified at the inlet. Taking advantage of the symmetry of the problem, only the square cross section shown in Fig. 2 is modeled. The physical domain of the CFD model has a high aspect ratio. Its dimensions are 37×37×1000 mm. The 3-D grid representing this domain consists of nodes that are clustered towards the porous walls to better represent the boundary layer that forms along them, and towards the inlet and the channel end sides to capture the velocity variations. A view of a part of the large grid is shown in Fig. 2. The

filter wall is modeled as a porous medium with Darcy's Law. For the present simulation a permeability of 1.5×10^{-12} m^2 was used. The solution takes around 20 minutes of CPU time on a Digital Alphastation 500 Series with 320 Mb RAM. The resulting velocity distribution and a 3-D view of the flow field are given in Fig. 3.

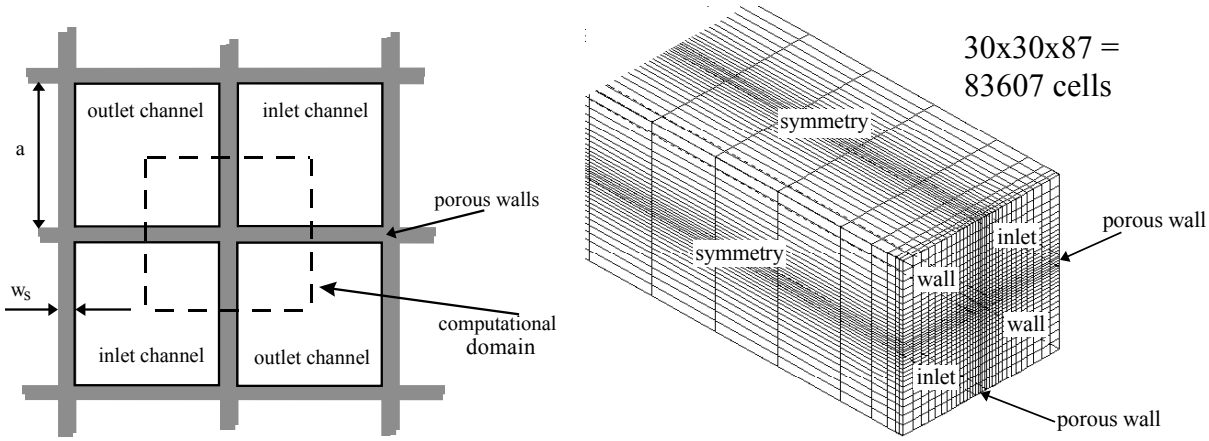

Figure 2 : Cross section of filter showing CFD model domain (left), and front part of grid (right)

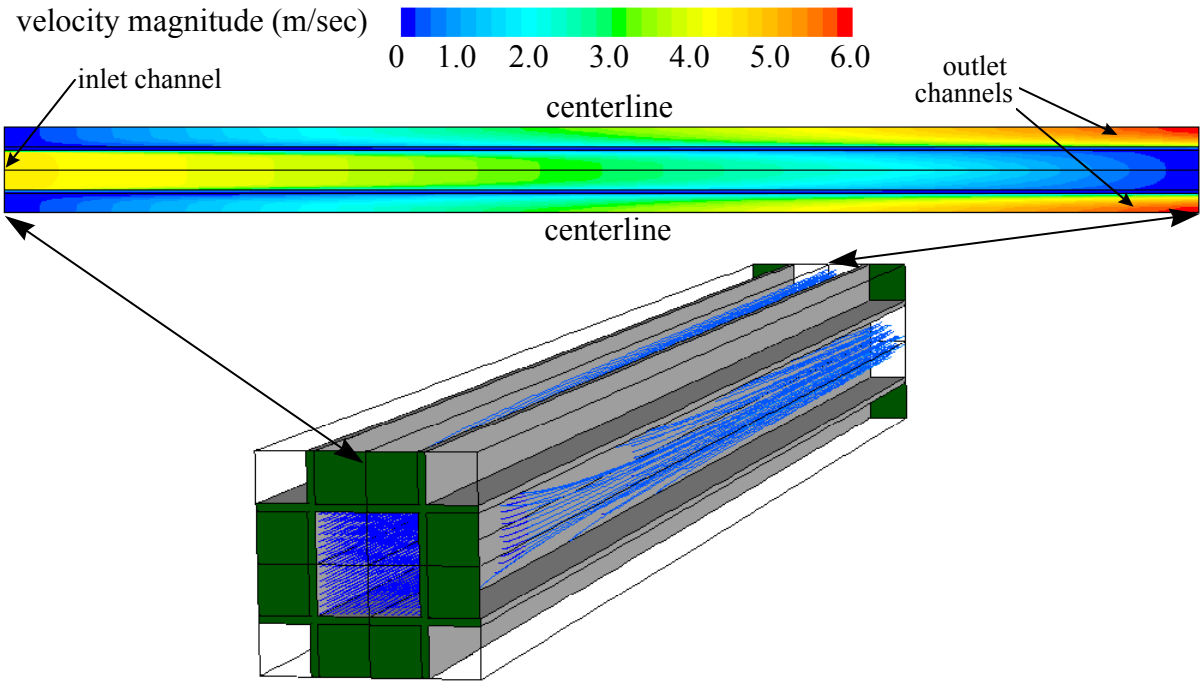

Figure 3 : Velocity magnitude contours at channel center plane (top) and flow streamlines

3.1.2. Transient CFD simulation

To examine the pulse jet cleaning process a transient simulation was performed, for the values listed in Table 2. With the computational resources available it was decided to simplify the geometry to an axisymmetric model [7], keeping the length and the filtration area the same. An imposed pressure difference of 3030 Pa (as obtained from the steady state solution) across the filter element drove the average wall flow of 4 cm/sec, which corresponds to normal filter operation. The cleaning jet nozzle was located as shown in Fig. 4.

Table 2 : Parameters used in the transient calculation

Pulse tube diameter (mm)	12
Pulse duration (msec)	100
Pulse maximum velocity (m/sec)	150
Pulse flow volume (Lit)	1.53
Pulse temperature (^{o}C)	20

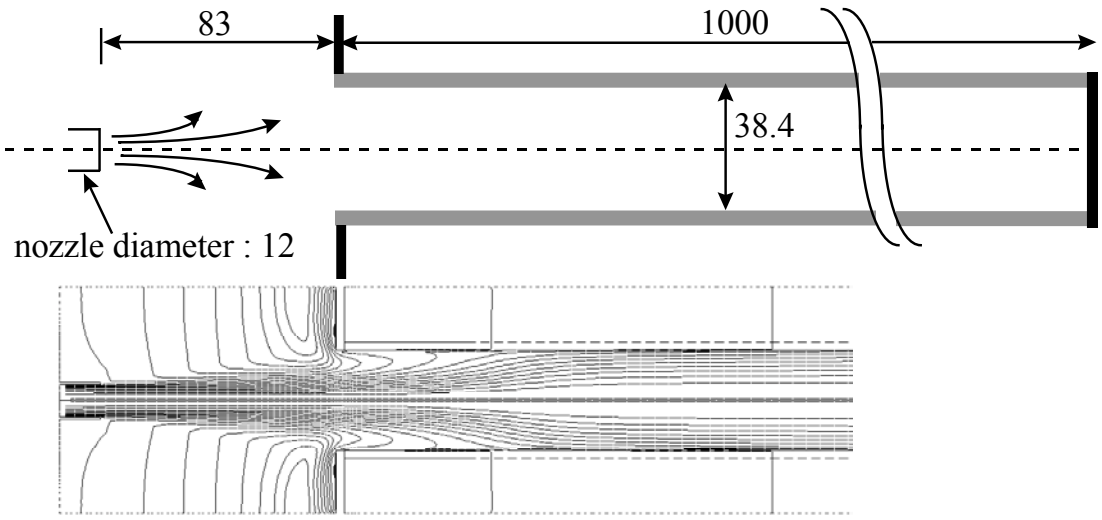

Figure 4 : Axisymmetric geometry for transient simulation, dimensions in mm (top) and jet streamlines 90 msec after pulsing (bottom).

The imposed time varying velocity profile for the cleaning jet is shown in Fig. 5. Nitrogen at room temperature (293 K) is used as cleaning gas. The resulting Mach number is around 0.5, so a compressible flow simulation was performed. A time step of 0.1 msec was used to capture the flow development in detail, and also to guarantee a stable solution progress. During pulse cleaning the maximum pressure drop reaches 32 kPa, while axial and wall velocities distributions are ploted in Figs. 5 and 6 at three time intervals. The back-pulse wall velocities are an order of magnitude higher than the operational filtration velocity, thus ensuring filter cleaning. The simulation also included the solution of the energy balance equation to study the effect of the cold jet on the hot ceramic filter during the cleaning procedure, see Fig. 7.

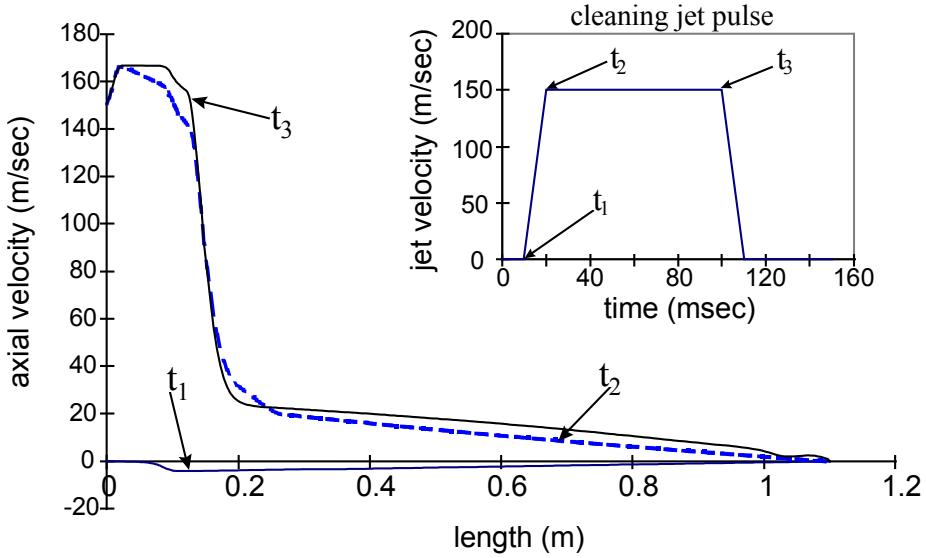

Figure 5 : Axial velocities along center line at three time intervals. Pulse jet profile used for the transient simulation (insert).

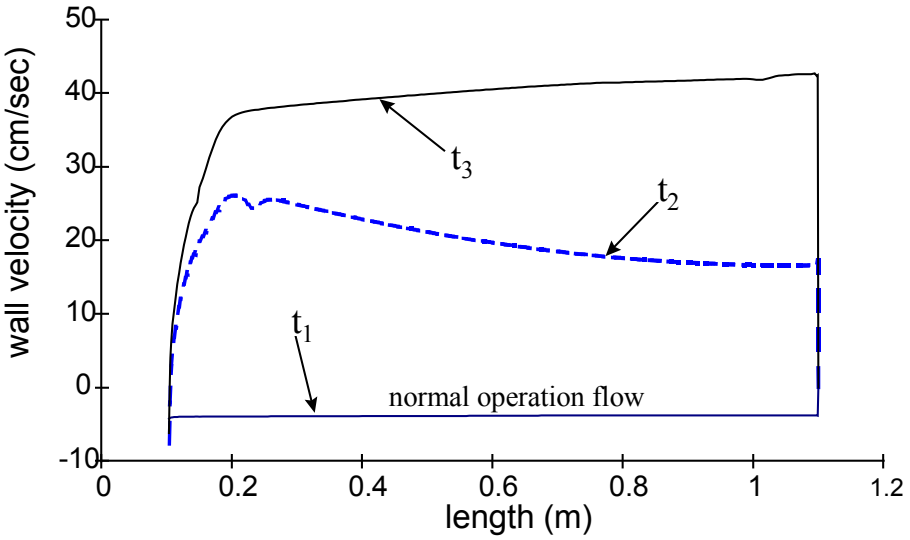

Figure 6 : Wall velocities at three time intervals

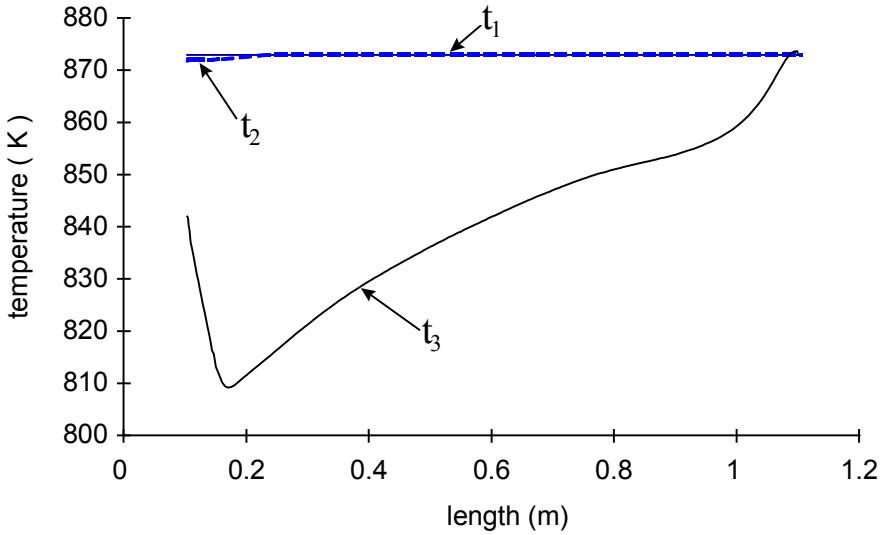

Figure 7 : Wall temperature at three time intervals

3.2 Analytic Model

Based on the the approach of Konstandopoulos & Johnson [8] addressing wall-flow particulate traps, an analytical solution to a 1-D filter channel flow model (Table 3) was extended to include non-Darcian (inertial) effects and was validated experimentally in [9].

Table 3 : 1-D analytical solution [8]

$\Delta P = \underbrace{\frac{\mu}{k}\frac{U_{in}a}{4L}w_s}_{Darcy} + \underbrace{\frac{3}{2}\frac{\mu F_1}{a^2}U_{in}L}_{frictional}$	$\hat{u}_w(\hat{x}) = c_1 g_1 e^{g_1 \hat{x}} + c_2 g_2 e^{g_2 \hat{x}}$
$\hat{u}_1(\hat{x}) = \frac{1}{2} - c_1 e^{g_1 \hat{x}} - c_2 e^{g_2 \hat{x}}$	$\hat{u}_2(\hat{x}) = \frac{1}{2} + c_1 e^{g_1 \hat{x}} + c_2 e^{g_2 \hat{x}}$

$g_1 = A_1 - \sqrt{A_1^2 + 2A_2}$ $g_2 = A_1 + \sqrt{A_1^2 + 2A_2}$ $c_1 = -\frac{1}{2} - c_2$ $c_2 = \frac{1}{2}\left[\frac{e^{g_1}+1}{e^{g_2}-e^{g_1}}\right]$	$A_1 = \frac{k}{\alpha w_s}\frac{4L}{\alpha}Re$ $A_2 = 4F\frac{k}{\alpha w_s}\left(\frac{L}{\alpha}\right)^2$ $F=28.454$

Although this analysis is valid for laminar channel flow, it is shown in Fig. 8 to be in very good agreement with the present 3-D CFD results due to the fact that for the operational conditions presently examined, the pressure drop is equivalent to that of a porous medium with the same total filtration area and thickness as the filter wall, and frictional losses are overwhelmed by the porous medium resistance contribution.

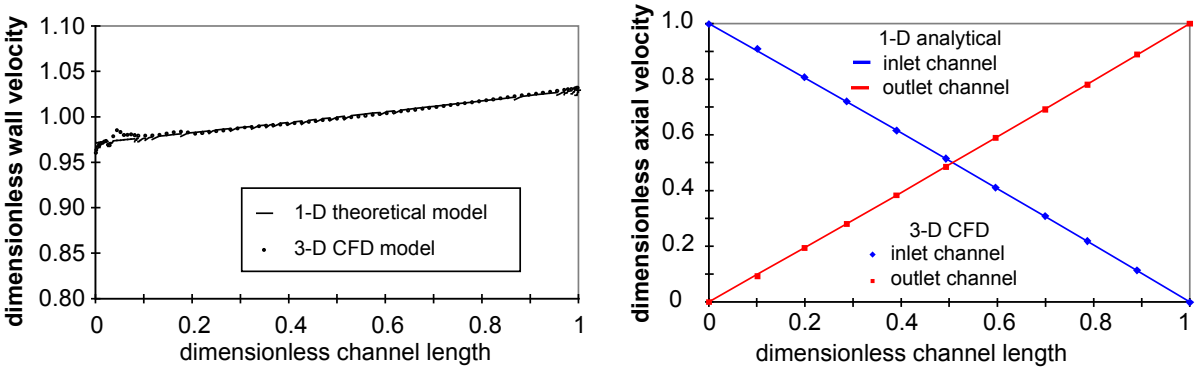

Figure 8 : wall velocity and channel axial velocities

4. Structural Analysis

The preliminary filter design described in Section 2 was subjected to finite element analysis in order to assess its structural integrity under loading and back-pulsing conditions. The critical basic design considerations are the tensional stress concentrations at the inner corner area of the square shaped filter tubes during gas flow. The position of the corners of each element is fixed (in contact with neighbor elements). A Modulus of elasticity of 85 GPa and a Poisson's ratio of 0.16 were used (characteristic values of silicon carbide, SiC). The load on the filter wall originating from the gas flow is regarded as uniform and isostatic. Two cases have been investigated; A) two dimensional; that is infinite length of the tubes with free ends. B) Fixed ends (simulating worst case in a rigid manifold), with a 10 mm length. The radius of curvature in the inside

corner has been varied from "zero" to 5 mm. It is seen in Figure 9, that even in the most critical case, that is "zero" curvature in the corners, the tensional stresses do not exceed 0.75 MPa which is considerably below the actual bending strength of most porous ceramics appropriate for the relevant type of filter application. A linear extrapolation to higher pressure gradients (which is reasonable) reveals that the upper tolerable pressure drop is in the region of several hundred kPa for SiC. Figure 9 reveals that fixation of the ends does not invoke problems. Tensional stresses at the fixed base are less than 0.3 MPa.

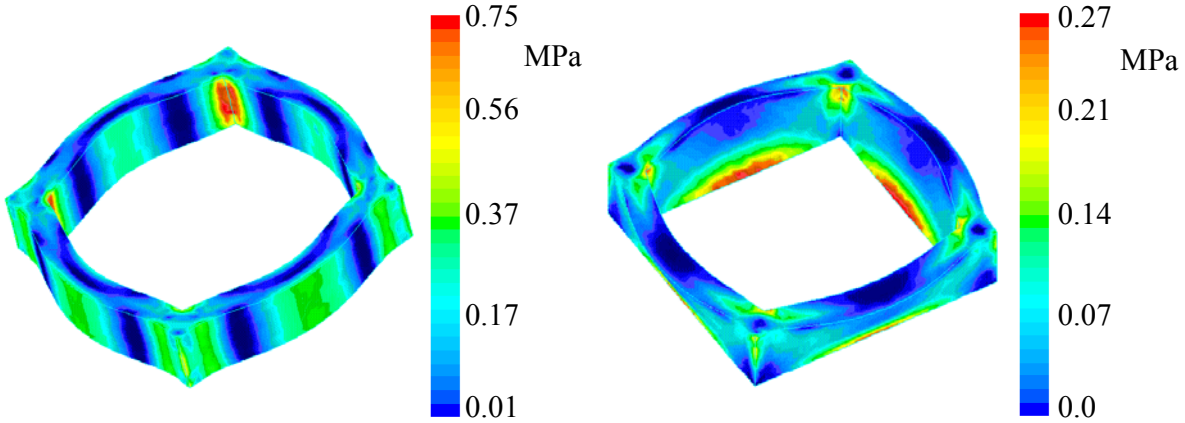

Figure 9 : Von Mises stress contours for “free” filter segment (left) and for fixed end segment (right) with deformations magnified by 4000.

5. Experimental

Ceramic filter materials are preferred when the process environment contains hot gases with a low oxygen content and has the possibility of a high sulfur content. In the present study the filter elements are considered to be extrudable advanced ceramics, such as silicon carbide (SiC) which has a number of advantages including superior high temperature strength (especially the non-clay bonded type of SiC). In addition, other ceramics such as cordierite or aluminum titanate, can also be used depending on hot gas composition and particulate characteristics.

As part of filter material development, filter coupons (disks) from SiC and cordierite have been extruded for testing. In addition, an alumina (Al_2O_3) membrane was deposited with a spray technique on a SiC filter coupon (for superior filtration performance). The SiC disks have pores in the size range from 25-40 microns and porosity in the range 45-50%. The pores of cordierite disks are in the size range from 35-50 microns and the porosity is in the range 50-55%. The filter coupons were tested for their permeability in a laboratory testing rig.

For testing the different filter materials, a hot gas flow rig has been constructed (Fig. 10), and it is currently under preliminary testing. Afterwards, it will be committed for testing the filter samples with respect to their behavior under

normal flow conditions and reverse pulse cleaning conditions. The experimental facility is designed to operate at a maximum pressure of 10 bar. The test section incorporates a filter holder which allows a 40 mm filter disk diameter to be exposed to the flow and it is heated to the desired temperature by means of a furnace with maximum operating temperature of 1000 ^{o}C. The filter testing flow rig is instrumented with particle measuring instrumentation which provides continuous, on-line measurement of the particle size, concentration and velocity, upstream and downstream of the filter.

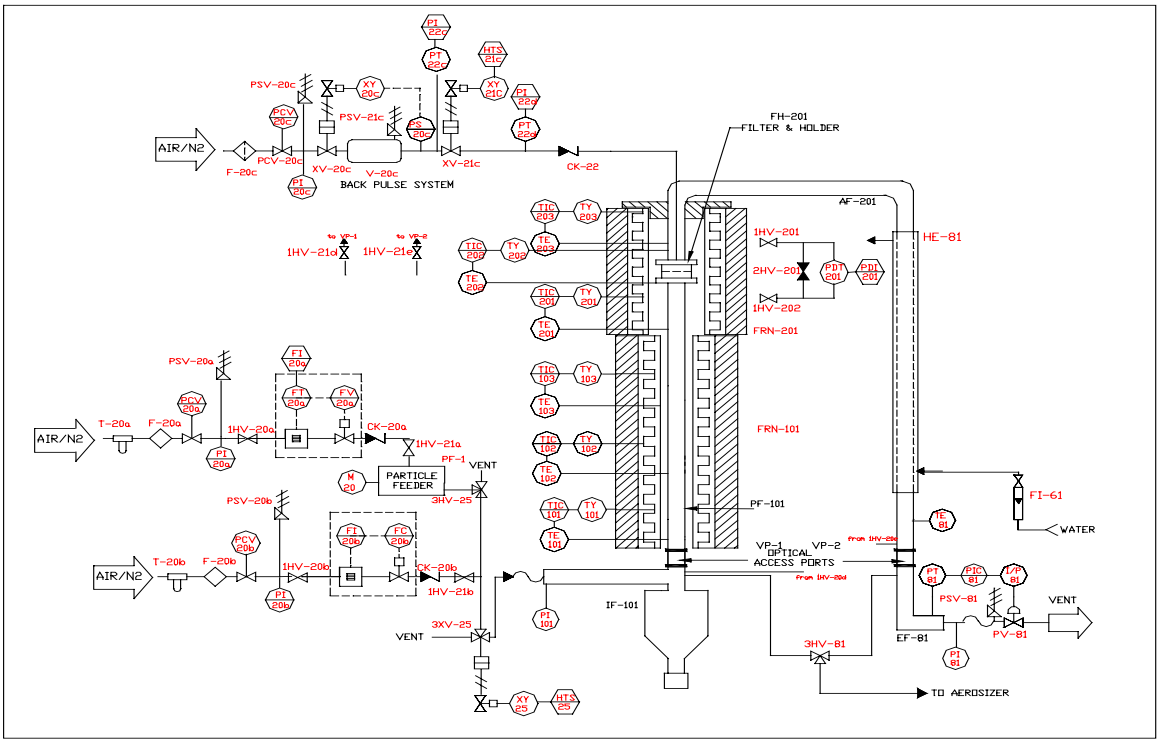

Figure 10: Experimental set-up

The filter coupons were tested with respect to their permeability, under cold flow conditions (20°C), using N_2 gas, in the flow rig of Fig. 10. The measured permeability in the case of SiC filter with Al_2O_3 membrane refers to the effective permeability k_{eff} of the filter substrate plus the membrane. The results of permeability measurements are shown in Figs. 11 and 12.

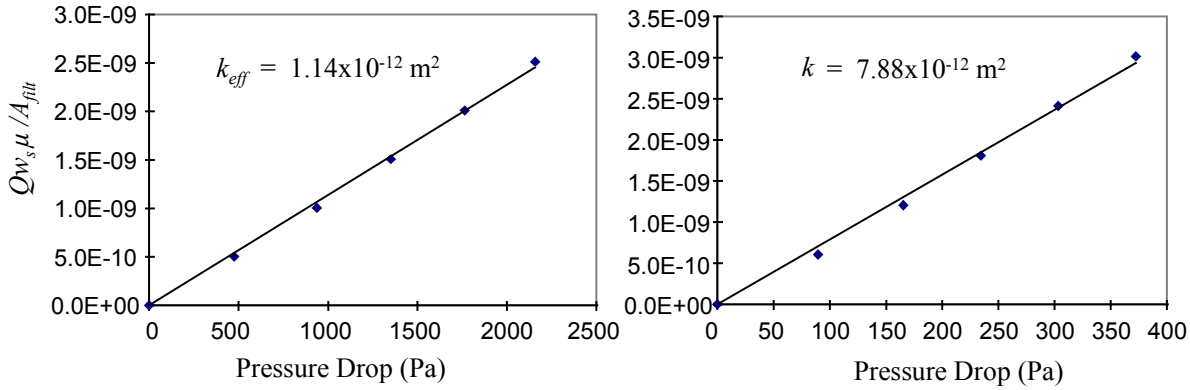

Figure 11 : Permeability measurements of SiC filter with Al_2O_3 membrane (left) and without membrane (right)

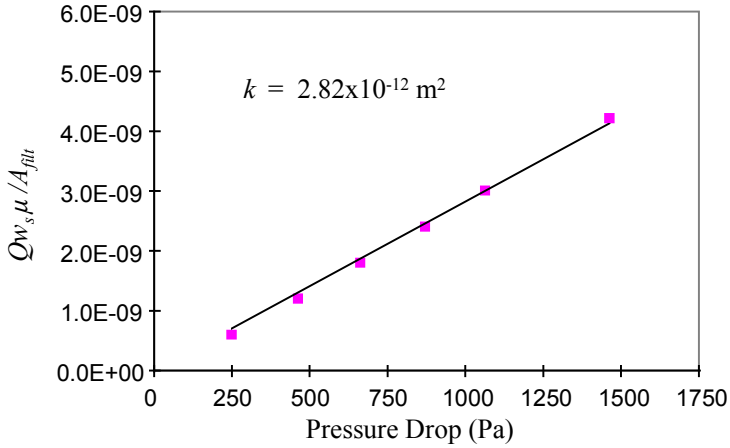

Figure 12: Permeability measurement of cordierite filter

It is of interest to comment on the findings of [10] regarding the influence of temperature on the effective permeability of a membrane coated cordierite honeycomb wall-flow filter. In that study it was shown that the pressure drop did not rise as predicted by the continuum theory of [8] but it exhibited a less dramatic rise as a function of temperature (see Fig. 13). However as already discussed in [8] at the temperatures under study and for the membrane pore sizes involved (typically less than a micron) the continuum theory (Darcy's law) does not hold any more and it is necessary to introduce slip-flow corrections in the evaluation of porous media permeabilities. This is shown by the continuous line in Fig. 13 where through the use of a simple correction factor similar to the familiar Stokes-Cuningham drag correction factor [11], and a resistance series treatment of the membrane plus filter substrate porous media, we can describe accurately the data of [10], as suggested originally in [8].

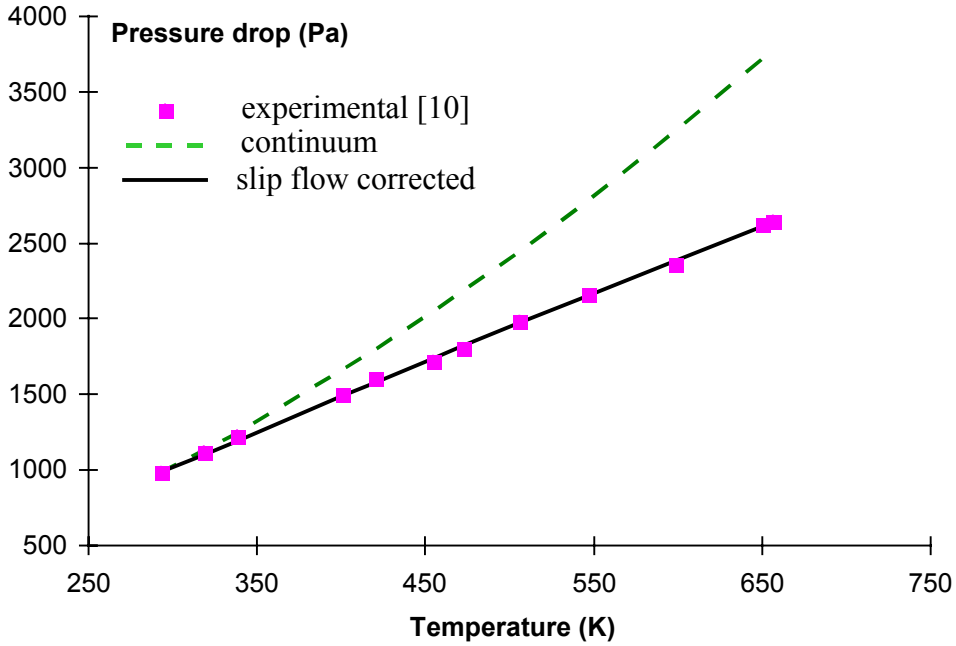

Figure 13 : Effect of temperature on pressure drop of the filter in [10].

6. Conclusions

Using CFD simulations, properly validated analytic models and finite element analysis, we have developed a methodology for optimal sizing of the novel assembled filter honeycomb. In addition suitable ceramic material formulations have been manufactured and are currently under testing in order to realize a pilot-scale prototype filter unit that promises to deliver substantial benefits to the hot-gas cleanup field compared to state-of-the-art technology.

Acknowledgments
This work has been supported in part by the European Commission (DG XII) under the framework of the JOULE-THERMIE III programme (Contract No. JOF3-CT97-0047).

References

1. Clift R. and Seville J.P.K, **Gas Cleaning at High Temperatures**, *Second International Symposium and Exhibition on Gas Cleaning at High Temperatures*, University of Surrey, 1993
2. Schmidt E., Gang P., Pilz T. & Dittler A., **High Temperature Gas Cleaning** *Third International Symposium and Exhibition on Gas Cleaning at High Temperatures*, University of Karlsruhe, 1996
3. Seville J.P.K., **Gas Cleaning in Demanding Applications**, Blackie Academic & Professional, 1997
4. Alvin, (1996) "Advanced Ceramic Materials for Use in High-Temperature Particulate Removal Systems" *Ind. Eng. Chem. Res.*, Vol. 35, pp. 3384-3398

5. Alvin, T.E., Lippert, and J.E. Lane, (1991) "Assessment of porous Ceramic Materials for Hot Gas Filtration Applications" *Ceramic Bulletin*, Vol. 70, No.9, pp. 1491-1498
6. Fluent.Inc, "Fluent 4.4 User Guide", June 1997
7. Christ A. & Renz U. "Numerical Simulation of Single Ceramic Filter Element Cleaning", High Temperature Gas Cleaning pp. 728-739, University of Karlsruhe, 1996
8. Konstandopoulos A.G., Johnson J. H. "Wall-Flow Diesel Particulate Filters - Their Pressure drop and Collection Efficiency" *SAE Trans*. 98 sec. 3 *(J. Engines)* Paper 890405, pp. 625-647, 1989
9. Konstandopoulos A. G., Skaperdas E., Warren J. & Allansson R. "Optimized Filter Design and Selection Criteria for Continuously Regenerating Diesel Particulate Traps" *SAE Paper* 1999-01-0468
10. Kwetkus B. A. & Egli W. "The Ceramic Monolithic Filter Module : Filtration Properties and DeNOx Potential", in High Temperature Gas Cleaning pp. 278-290, University of Karlsruhe, 1996
11. Friedlander S.K., **Smoke Dust and Haze - Fundamentals of Aerosol Behavior**, Wiley, NY, 1977

Definitions

a : channel width
A_{filt} : filtration area
D : assembled filter diameter
F : factor equal to 28.454
k : permeability of substrate
k_{eff} : effective permeability
k_m : permeability of membrane
L : filter height or channel length
M : jet Mach number
μ : exhaust dynamic viscosity
Q : volumetric flow rate
Re : channel entrance Reynolds number
u_1, u_2 : inlet and outlet axial velocities
u_w : wall velocity
U_{in} : inlet cell entrance velocity
V : filter volume
w_s: filter wall thickness
w_m : membrane thickness
x : channel axial coordinate
ρ : exhaust gas density